Bandwidth Characteristics of Inhomogeneous T-Septum Waveguides

PRADIP KUMAR SAHA AND GOPA GUHA MAZUMDER

Abstract—**Rectangular waveguides with T-shaped septa were recently shown to have superior characteristics compared to conventional ridged guides. Here the dispersion equations of the hybrid modes of an inhomogeneously filled septum guide have been determined by the Ritz–Galerkin technique. Results of numerical computations indicate that with dielectric filling of the septum gap, further enhancement of the cutoff wavelength of the lowest mode and the bandwidth with respect to the next higher mode is possible.**

I. Introduction

RECENTLY the authors proposed rectangular waveguides with one or two T-shaped septa as superior alternatives to conventional single- and double-ridged guides [1], [2]. These structures exhibit broader bandwidth and larger cutoff wavelength of the dominant TE_{10} mode. Other workers have subsequently examined the T-septum guides, supported the original results, and deduced more information [3], [4].

In this paper we consider inhomogeneously filled double and single T-septum guides (henceforth referred to as IDTSG's and ISTSG's, respectively), shown in Fig. 1(a) and (b). In particular we wish to calculate the effect of filling the septum gap region with a dielectric on the cutoff wavelength and bandwidth. Magerl [5] showed theoretically that loading the gap of a double-ridged guide (DRG) with a dielectric slab substantially enhances both the TE_{10} cutoff wavelength and TE_{10}–TE_{20} separation. However, this determination of the dispersion equation for TE modes is valid only at cutoff [6] since, strictly speaking, the modes should be hybrid.

We have analyzed the ISTSG by the Ritz–Galerkin technique as in [1] and [2] but in terms of hybrid fields. Since in the case of the IDTSG we are interested in the first two hybrid modes with electric symmetry along the plane bisecting the gap, it is sufficient to determine the dispersion equations of the hybrid modes of the ISTSG. The results presented here indicate a broader range of parameters with dielectric loading of the septum gap compared to air-filled DTSG's and STSG's.

II. Inhomogeneous T-Septum Guides

The inhomogeneously filled double and single T-septum guides are shown in Fig. 1(a) and (b). The actual configuration analyzed here—a half section of an ISTSG—is shown in Fig. 1(c). In particular we are interested in $\epsilon_{r2} = \epsilon_{r3} = 1$ and $\epsilon_{r1} > 1$.

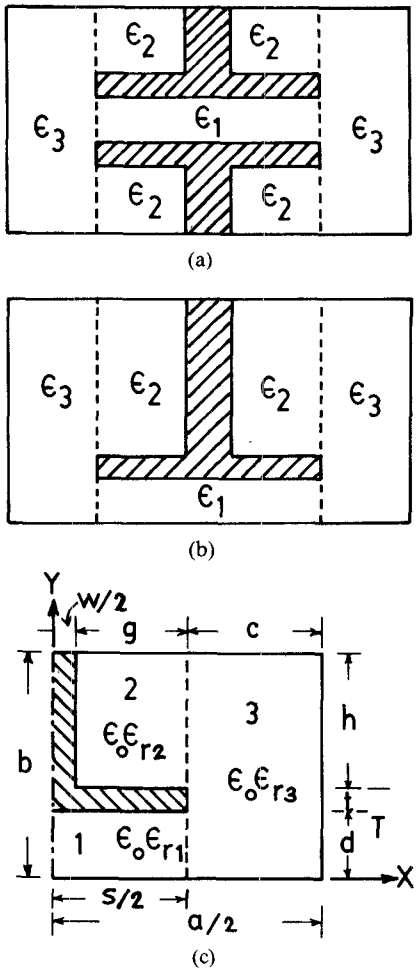

Fig. 1. (a) Inhomogeneous double T-septum guide (IDTSG). (b) Inhomogeneous single T-septum guide (ISTSG). (c) One half of the cross section of ISTSG.

III. Analysis

The formulation of the problem is similar to that in [1] except that both the y and z components of the electric and magnetic fields are used in field matching. We therefore mention only the steps and give the final matrix eigenvalue equations from which the dispersion characteristics can be calculated.

1) The electric and magnetic scalar potentials in different regions are written in appropriate expanded forms.

Manuscript received July 20, 1988; revised December 19, 1988.

The authors are with the Institute of Radio Physics and Electronics, 92 Acharya Prafulla Chandra Road, Calcutta 700 009, India.

IEEE Log Number 8927167.

0018-9480/89/0600-1021$01.00 ©1989 IEEE

2) The y and z components of the electric and magnetic fields in three regions are written in terms of the scalar potentials.

3) The unknown transverse and longitudinal electric fields over the apertures at $x = s/2$ are denoted, respectively, by

(i) $E_{y1}(y)$ and $E_{z1}(y)$, $0 \leqslant y \leqslant d$

(ii) $E_{y2}(y)$ and $E_{z2}(y)$, $T \leqslant y \leqslant b$.

4) Four equations are obtained by matching the y and z components of the H field over the apertures.

5) By matching the y and z components of the E field, the expansion coefficients of the scalar potentials are expressed in terms of $E_{y1,2}(y)$ and $E_{z1,2}(y)$.

6) Substituting the expressions obtained in step 5 into the equations obtained in step 4, four coupled integral equations in $E_{y1,2}$ and $E_{z1,2}$ are formed.

7) The unknown aperture fields are expanded as

$$E_{y1} = \sum_{i=0}^{N_1} A_{1i} \cos \frac{i\pi}{d}(y-d) \tag{1}$$

$$E_{z1} = \sum_{i=1}^{N_1} B_{1i} \sin \frac{i\pi}{d}(y-d) \tag{2}$$

$$E_{y2} = \sum_{i=0}^{N_2} A_{2i} \cos \frac{i\pi}{h}(y-T) \tag{3}$$

$$E_{z2} = \sum_{i=1}^{N_2} B_{2i} \sin \frac{i\pi}{h}(y-T). \tag{4}$$

8) Using (1)–(4) the integral equations obtained in step 6 are transformed into four sets of homogeneous equations in A_{1i}, B_{1i}, A_{2i} and B_{2i} (see the Appendix).

Equations (A1)–(A4) can be put into matrix form:

$$[H(k_0, \beta)][\underline{A}_1^T \underline{B}_1^T \underline{A}_2^T \underline{B}_2^T]^T = 0 \tag{5}$$

where H is a square matrix of size $2(N_1 + N_2 + 1)$. The dispersion characteristics can be determined from the roots of

$$\det[H(k_0, \beta)] = 0. \tag{6}$$

Setting $\beta = 0$ at cutoff, (6) splits into two decoupled equations:

$$[H'(k_c)][\underline{A}_1^T \underline{A}_2^T]^T = 0 \tag{7}$$

$$[H''(k_c)][\underline{B}_1^T \underline{B}_2^T]^T = 0 \tag{8}$$

where k_c is the cutoff wavenumber. The eigenvalue equations

$$\det[H'(k_c)] = 0 \tag{9}$$

$$\det[H''(k_c)] = 0 \tag{10}$$

yield the cutoff wavelengths of HE and EH type modes, respectively

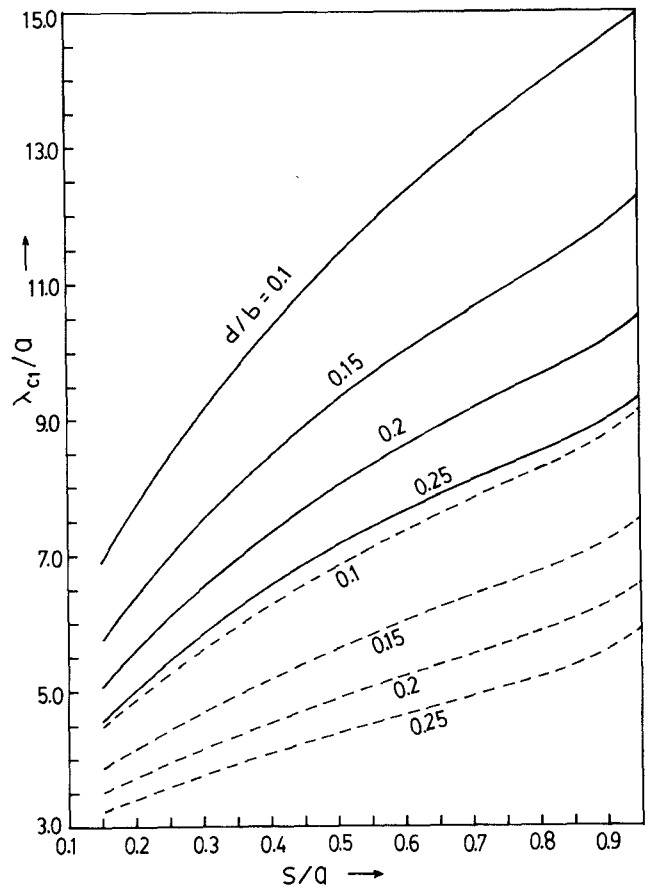

Fig. 2. Variation of normalized cutoff wavelength (λ_{c1}/a) of HE_1 mode: $b/a = 0.5$, $w/a = 0.1$, $t/b = 0.05$ —— IDTSG ($\epsilon_{r1} = 3.0$, $\epsilon_{r2} = \epsilon_{r3} = 1.0$); ----- DTSG ($\epsilon_{r1} = \epsilon_{r2} = \epsilon_{r3} = 1.0$).

IV. Results of Numerical Computation

The first few hybrid modes of inhomogeneous T-septum guides are HE modes. The dominant and the next higher mode, both having electric symmetry along the X axis and magnetic and electric symmetry, respectively, along the Y axis, will be designated as HE_1 and HE_2, respectively. The corresponding cutoff wavelengths are designated as λ_{c1} and λ_{c2}, so that $\lambda_{c1}/\lambda_{c2}$ is the modal separation.

Computation of λ_{c1} and λ_{c2} from the solution of (9) was carried out with $N_1 = N_2 = 10$ and $L = 15$. The dimensional parameters are the same as those of the DTSG and the STSG in [1] and [2]. Figs. 2 and 3 show the variation of λ_{c1}/a with s/a for different values of d/b when the septum gap (region 1) is filled with a dielectric of $\epsilon_{r1} = 3.0$ and $\epsilon_{r2} = \epsilon_{r3} = 1.0$. Also shown in the figures are the corresponding curves of the TE_{10} modes in the DTSG and the STSG. As in the case of homogeneous T-septum guides, λ_{c1}/a increases continuously with s/a. The dielectric loading of the gap with $\epsilon_{r1} = 3.0$ increases the HE_1 cutoff wavelength by 67 percent for an IDTSG and by 69 percent for an ISTSG when $s/a = 0.9$ and $d/b = 0.1$.

The enhancement of λ_{c2}/a of the HE_2 mode is, however, smaller, as can be seen from Figs. 4 and 5. As a result, the modal separation $\lambda_{c1}/\lambda_{c2}$ is also increased by the dielectric loading. It may also be noted here that with the dielectric loading the dependence of λ_{c2}/a on d/b

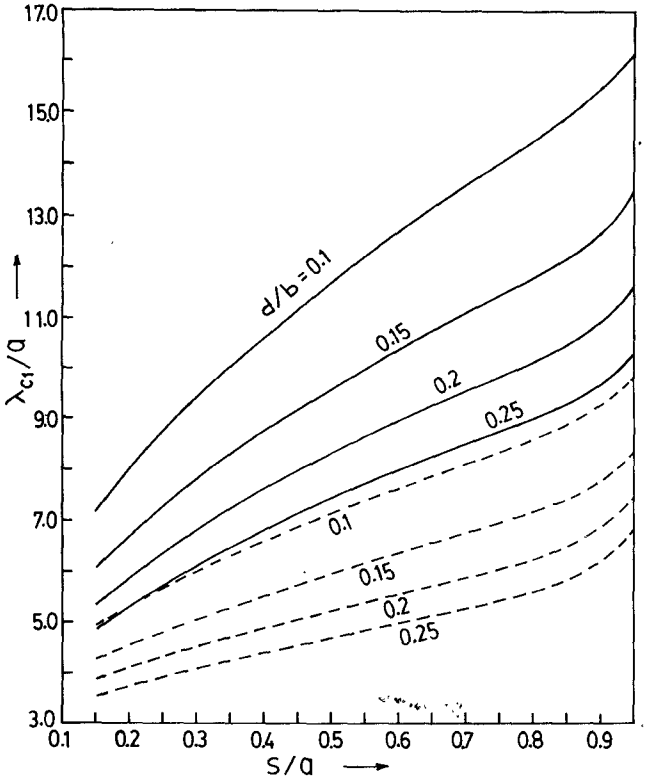

Fig. 3. Variation of normalized cutoff wavelength (λ_{c1}/a) of HE_1 mode: $b/a = 0.45$, $w/a = 0.1$, $t/b = 0.05$. —— ISTSG ($\epsilon_{r1} = 3.0$, $\epsilon_{r2} = \epsilon_{r3} = 1.0$); ---- STSG ($\epsilon_{r1} = \epsilon_{r2} = \epsilon_{r3} = 1.0$).

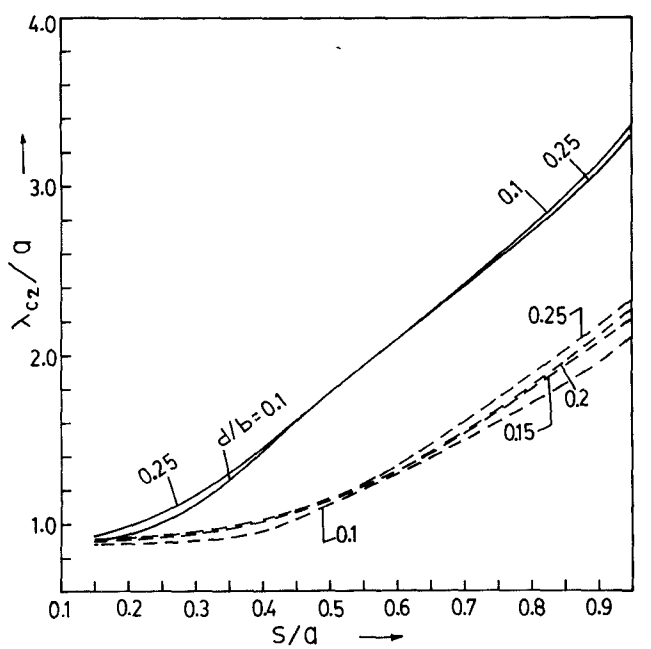

Fig. 4. Variation of normalized cutoff wavelength (λ_{c2}/a) of HE_2 mode: $b/a = 0.5$, $w/a = 0.1$, $t/b = 0.05$. —— IDTSG ($\epsilon_{r1} = 3.0$, $\epsilon_{r2} = \epsilon_{r3} = 1.0$); ---- DTSG ($\epsilon_{r1} = \epsilon_{r2} = \epsilon_{r3} = 1.0$).

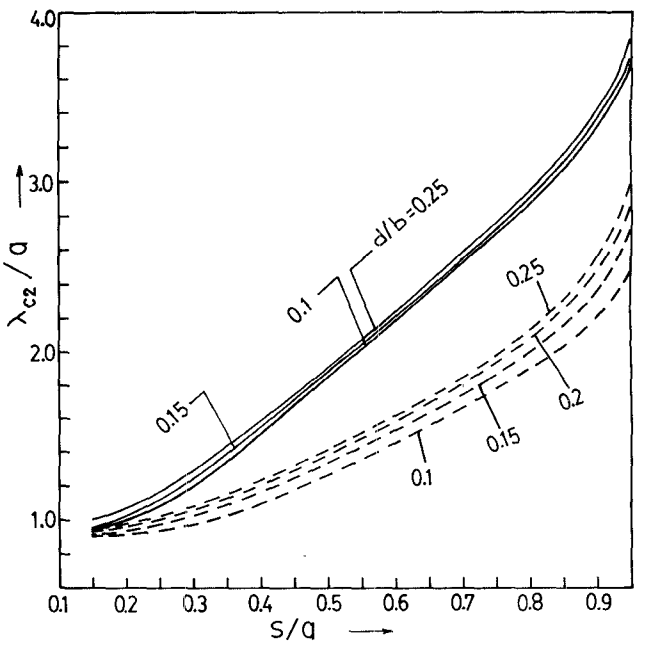

Fig. 5. Variation of normalized cutoff wavelength (λ_{c2}/a) of HE_2 mode: $b/a = 0.45$, $w/a = 0.1$, $t/b = 0.05$. —— ISTSG ($\epsilon_{r1} = 3.0$, $\epsilon_{r2} = \epsilon_{r3} = 1.0$); ---- STSG ($\epsilon_{r1} = \epsilon_{r2} = \epsilon_{r3} = 1.0$).

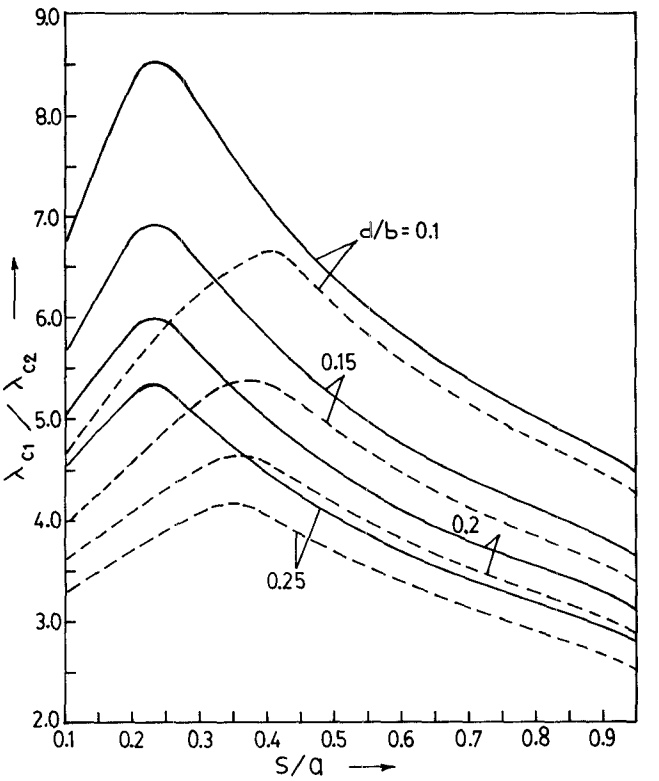

Fig. 6. Bandwidth characteristics: variation of ($\lambda_{c1}/\lambda_{c2}$) $b/a = 0.5$, $w/a = 0.1$, $t/b = 0.05$. —— IDTSG ($\epsilon_{r1} = 3.0$, $\epsilon_{r2} = \epsilon_{r3} = 1.0$); ---- DTSG ($\epsilon_{r1} = \epsilon_{r2} = \epsilon_{r3} = 1.0$).

has decreased to some extent. The variation of $\lambda_{c1}/\lambda_{c2}$ is shown in Figs. 6 and 7. Another feature to be observed is that the dielectric loading shifts the bandwidth peaks to smaller values of s/a than is the case with air-filled T-septum guides. For $\epsilon_{r1} = 3.0$ and $d/b = 0.1$, the peak shifts to $s/a = 0.23$ for the IDTSG from $s/a = 0.41$ for the DTSG and to $s/a = 0.23$ for the ISTSG from $s/a = 0.33$ for the STSG. The magnitude of this shift due to dielectric loading increases as the relative permittivity ϵ_{r1} increases. This is shown in Figs. 8 and 9, where the variation of $\lambda_{c1}/\lambda_{c2}$ with s/a is plotted for $d/b = 0.1$ and various values of ϵ_{r1} from 1 to 10.

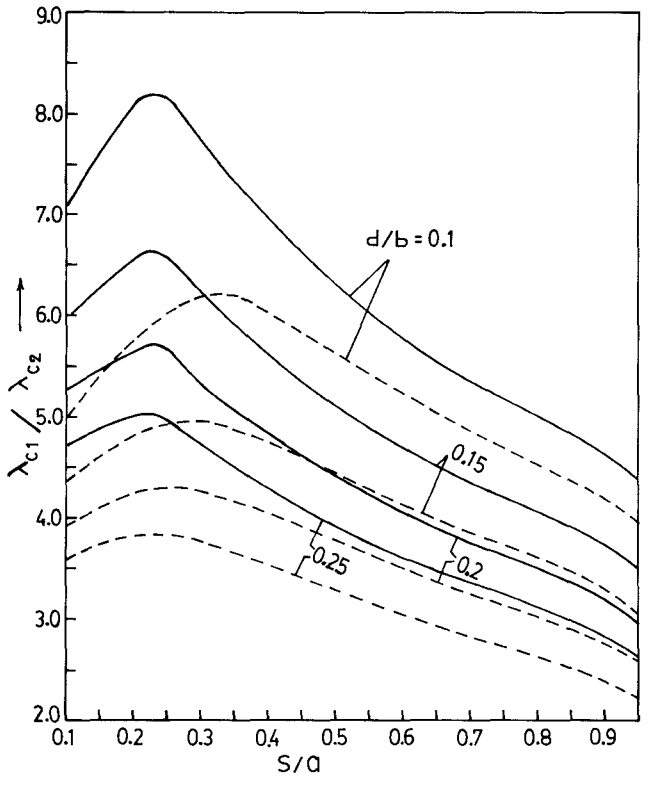

Fig. 7. Bandwidth characteristics: variation of $(\lambda_{c1}/\lambda_{c2})$. $b/a = 0.45$, $w/a = 0.1$, $t/b = 0.05$. ——— ISTSG ($\epsilon_{r1} = 3.0$, $\epsilon_{r2} = \epsilon_{r3} = 1.0$); ---- STSG ($\epsilon_{r1} = \epsilon_{r2} = \epsilon_{r3} = 1.0$).

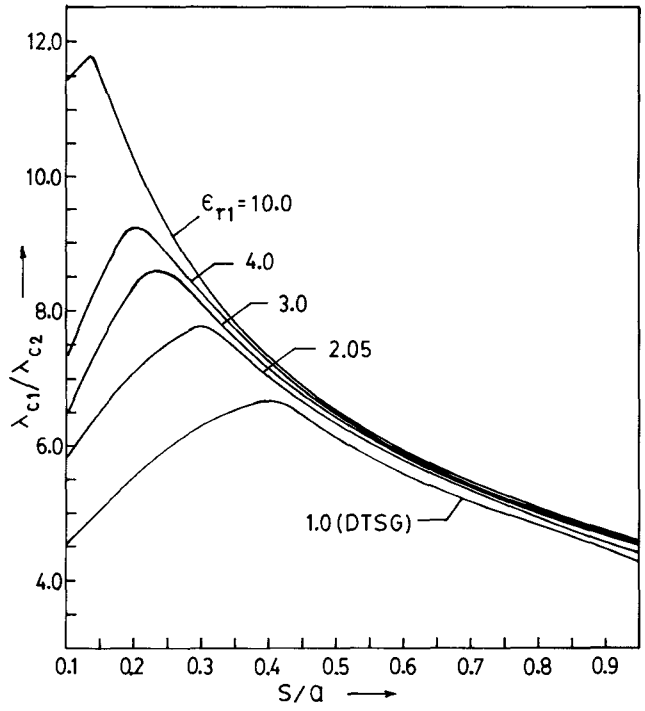

Fig. 8. Variation of modal separation $(\lambda_{c1}/\lambda_{c2})$ of IDTSG with dielectric loading (ϵ_{r1}) of septum gap: $b/a = 0.5$, $w/a = 0.1$, $t/b = 0.05$, $d/b = 0.1$, $\epsilon_{r2} = \epsilon_{r3} = 1.0$.

Similar features were observed by Magerl [5] in the case of gap-filled DRG. According to [5], the bandwidth peak of inhomogeneous DRG occurs at a value of s/a that depends on ϵ_{r1} but not on d/b. For the IDTSG and ISTSG also the value of s/a corresponding to the bandwidth peak decreases with increasing ϵ_{r1}, but for a particular ϵ_{r1} the peak appears at the same value of s/a for all values of d/b. For homogeneous ridged and septum guides, however, the bandwidth peak occurs at s/a values that decrease with increasing d/b.

V. Conclusions

We have derived the dispersion equations of the hybrid modes in an inhomogeneously filled single T-septum guide and from these have computed the effect of dielectric loading of the gap on the cutoff wavelength of the dominant HE_1 mode and its bandwidth with respect to the next higher HE_2 mode in both an IDTSG and an ISTSG. Both these parameters are enhanced by the dielectric loading in comparison with the TE_{10} cutoff wavelength and TE_{10}–TE_{20} separation in the air-filled septum guides. Our results also indicate that just as the DTSG and STSG have improved characteristics compared to double- and single-ridged guides, respectively, the inhomogeneous septum guides, too, have characteristics superior to those of gap-filled ridged guides.

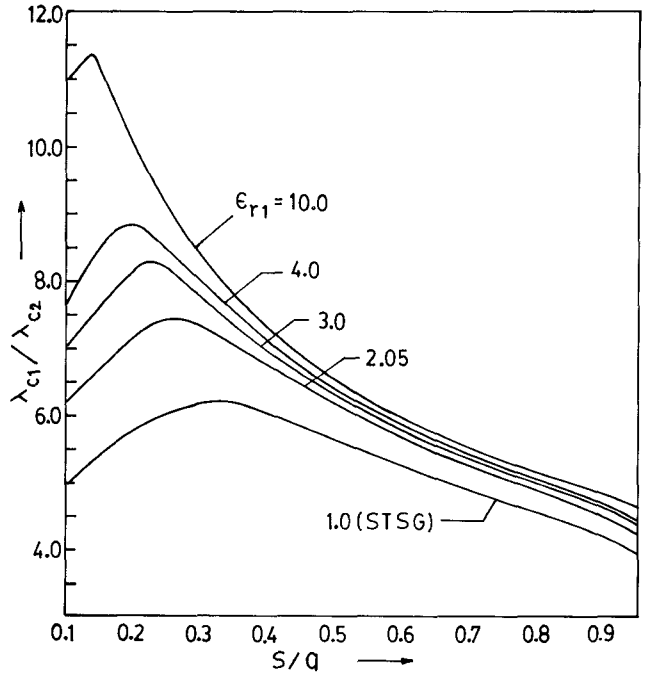

Fig. 9. Variation of modal separation $(\lambda_{c1}/\lambda_{c2})$ of ISTSG with dielectric loading (ϵ_{r1}) of septum gap: $b/a = 0.45$, $w/a = 0.1$, $t/b = 0.05$, $d/b = 0.1$, $\epsilon_{r2} = \epsilon_{r3} = 1.0$.

Appendix

The four sets of homogeneous equations in A_{1t}, B_{1t}, A_{2t}, and B_{2t}, the coefficients of expansion in (1)–(4), are

given below:

$$\sum_{i=0}^{N_1} A_{1i}\left\{T_1 \sum_{l=0}^{L} U_{1pl}U_{1il}\phi_l|\epsilon_l + \delta_{ip}\left(\epsilon_p k_{c1}^2 sd\theta_{1p}|2\right)\right\} + j\sum_{i=1}^{N_1} B_{1i}\left\{T_2 \sum_{l=1}^{L} lU_{1pl}V_{1il}\phi_l + \delta_{ip}\left(p\pi\bar{\beta}k_0 s\theta_{1p}|4\right)\right\} + \sum_{i=0}^{N_2} A_{2i}\left\{T_1 \sum_{l=0}^{L} U_{1pl}U_{2il}\phi_l|\epsilon_l\right\} + j\sum_{i=1}^{N_2} B_{2i}\left\{T_2 \sum_{l=1}^{L} lU_{1pl}V_{2il}\phi_l\right\} = 0, \quad p = 0,1,2,\cdots,N_1 \quad \text{(A1)}$$

$$\sum_{i=0}^{N_1} A_{1i}\left\{T_3 \sum_{l=1}^{L} lV_{1pl}U_{1il}\phi_l + \delta_{ip}\left(p\pi\bar{\beta}k_{c1}^2 k_{c3}^2 s\theta_{1p}|4\right)\right\} + j\sum_{i=1}^{N_1} B_{1i}\left\{k_0 k_{c1}^2 \sum_{l=1}^{L} V_{1pl}V_{1il}\alpha_l + \delta_{ip}k_0 k_{c3}^2\left(\epsilon_{r1}\sigma_{1p}d/s + \bar{\beta}^2(p\pi/d)^2 sd\theta_{1p}/4\right)\right\} + \sum_{i=0}^{N_2} A_{2i}\left\{T_3 \sum_{l=1}^{L} lV_{1pl}U_{2il}\phi_l\right\} + j\sum_{i=1}^{N_2} B_{2i}\left\{k_0 k_{c1}^2 \sum_{l=1}^{L} V_{1pl}V_{2il}\alpha_l\right\} = 0, \quad p = 1,2,\cdots,N_1 \quad \text{(A2)}$$

$$\sum_{i=0}^{N_1} A_{1i}\left\{T_1 \sum_{l=0}^{L} U_{2pl}U_{1il}\phi_l/\epsilon_l\right\} + j\sum_{i=1}^{N_1} B_{1i}\left\{T_2 \sum_{l=1}^{L} lU_{2pl}V_{1il}\phi_l\right\} + \sum_{i=0}^{N_2} A_{2i}\left\{T_1 \sum_{l=0}^{L} U_{2pl}U_{2il}\phi_l/\epsilon_l + \delta_{ip}\left(\epsilon_p k_{c2}^2 gh\theta_{2p}\right)\right\} + j\sum_{i=1}^{N_2} B_{2i}\left\{T_2 \sum_{l=1}^{L} lU_{2pl}V_{2il}\phi_l + \delta_{ip}\left(p\pi\bar{\beta}k_0 g\theta_{2p}/2\right)\right\} = 0, \quad p = 0,1,2,\cdots,N_2 \quad \text{(A3)}$$

$$\sum_{i=0}^{N_1} A_{1i}\left\{T_4 \sum_{l=1}^{L} lV_{2pl}U_{1il}\phi_l\right\} + j\sum_{i=1}^{N_1} B_{1i}\left\{k_0 k_{c2}^2 \sum_{l=1}^{L} V_{2pl}V_{1il}\alpha_l\right\} + \sum_{i=0}^{N_2} A_{2i}\left\{T_4 \sum_{l=1}^{L} lV_{2pl}U_{2il}\phi_l + \delta_{ip}\left(p\pi\bar{\beta}k_{c2}^2 k_{c3}^2 g\theta_{2p}/2\right)\right\} + j\sum_{i=1}^{N_2} B_{2i}\left\{k_0 k_{c2}^2 \sum_{l=1}^{L} V_{2pl}V_{2il}\alpha_l + \delta_{ip}k_0 k_{c3}^2\left(\epsilon_{r2}\sigma_{2p}h/2g + \bar{\beta}^2(p\pi/h)^2 gh\theta_{2p}/2\right)\right\} = 0, \quad p = 1,2,\cdots,N_2 \quad \text{(A4)}$$

where

$$T_0 = 2\pi\bar{\beta}c/b^2$$

$$\bar{\beta} = \beta/k_0$$

$$T_1 = k_{c3}^2 c/b$$

$$T_2 = T_0 k_0$$

$$T_3 = T_0 k_{c1}^2 k_{c3}^2$$

$$T_4 = T_0 k_{c2}^2 k_{c3}^2 \quad \text{(A5)}$$

$$\phi_l = \cot k_{x3l}c/k_{x3l}c$$

$$\psi_l = k_{x3l}c\cdot\cot k_{x3l}c \quad \text{(A6)}$$

$$\theta_{1p} = \begin{matrix}-\tan\\+\cot\end{matrix} k_{x1p}s/2/(k_{x1p}s/2)$$

$$\theta_{2p} = \cot k_{x2p}g/k_{x2p}g \quad \text{(A7)}$$

$$\sigma_{1p} = k_{x1p}s/2\left(\begin{matrix}-\tan\\+\cot\end{matrix} k_{x1p}s/2\right)$$

$$\sigma_{2p} = k_{x2p}g\cdot\cot k_{x2p}g \quad \text{(A8)}$$

$$\alpha_l = 2\epsilon_{r3}\psi_l/cb + \bar{\beta}^2(l\pi/b)^2 c\phi_l/2b \quad \text{(A9)}$$

$$k_{c1}^2 = (p\pi/d)^2 + k_{x1p}^2 = k_0^2(\epsilon_{r1} - \bar{\beta}^2)$$

$$k_{c2}^2 = (p\pi/h)^2 + k_{x2p}^2 = k_0^2(\epsilon_{r2} - \bar{\beta}^2)$$

$$k_{c3}^2 = (p\pi/b)^2 + k_{x3p}^2 = k_0^2(\epsilon_{r3} - \bar{\beta}^2)$$

$$\epsilon_p = 1(p=0), 1/2(p\neq 0). \quad \text{(A10)}$$

The upper and lower trigonometric functions correspond to magnetic and electric symmetry, respectively, along the Y axis in the gap (region 1):

$$U_{1ik} = \int_0^d \cos\frac{i\pi}{d}(y-d)\cos\frac{k\pi}{b}(y-b)\,dy \quad \text{(A11)}$$

$$V_{1ik} = \int_0^d \sin\frac{i\pi}{d}(y-d)\sin\frac{k\pi}{b}(y-b)\,dy \quad \text{(A12)}$$

$$U_{2ik} = \int_T^b \cos\frac{i\pi}{h}(y-T)\cos\frac{k\pi}{b}(y-b)\,dy \quad \text{(A13)}$$

$$V_{2ik} = \int_T^b \sin\frac{i\pi}{h}(y-T)\sin\frac{k\pi}{b}(y-b)\,dy. \quad \text{(A14)}$$

References

[1] G. Guha Mazumder and P. K. Saha, "A novel rectangular waveguide with double T-septum," *IEEE Trans. Microwave Theory Tech.*, vol. MTT-33, pp. 1235–1238, Nov. 1985.

[2] G. Guha Mazumder and P. K. Saha, "Rectangular waveguide with T-shaped septa," *IEEE Trans. Microwave Theory Tech.*, vol. MTT-35, pp. 201–204, Feb. 1987.

[3] Y. Zhang and W. T. Joines, "Some properties of T-septum waveguides," *IEEE Trans. Microwave Theory Tech.*, vol. MTT-35, pp. 769–775, Aug. 1987.
[4] Y. Zhang and W. T. Joines, "Attenuation and power handling capability of T-septum waveguides," *IEEE Trans. Microwave Theory Tech.*, vol. MTT-35, pp. 858–861, Sept. 1987.
[5] G. Magerl, "Ridged waveguide with inhomogeneous dielectric slab loading," *IEEE Trans. Microwave Theory Tech.*, vol. MTT-26, pp. 413–416, June 1978.
[6] C. W. Young and G. Magerl, "Comments on ridged waveguides with inhomogeneous dielectric slab loading," *IEEE Trans. Microwave Theory Tech.*, vol. MTT-26, p. 919, Nov. 1978.

Pradip Kumar Saha received the B.Sc. (hons.) degree in 1963, the M.Tech. degree in radiophysics and electronics in 1966 from Calcutta University, and the Ph.D. degree from the University of Leeds, England.

He has been on the teaching staff of the Institute of Radiophysics and Electronics, Calcutta University, since 1971. He is currently engaged in work on millimeter-wave and optical transmission media and microwave semiconductor sources.

Gopa Guha Mazumder was born in 1957. She obtained the B.Sc. (hons.), B.Tech., and M.Tech. degrees in radiophysics and electronics from Calcutta University in 1976, 1979, and 1982, respectively. In 1988 she completed a research program for the Ph.D. degree. Her field of interest is microwave and millimeter-wave transmission media.